Supporting Information

Solar Light Irradiated Photocatalytic Degradation of Model Dyes and Industrial Dyes by a Magnetic $CoFe_2O_4$-gC_3N_4 S-Scheme Heterojunction Photocatalyst

*Debika Gogoi, Priyanka Makkar, Narendra Nath Ghosh**

Nano-materials Lab, Department of Chemistry, Birla Institute of Technology and Science, Pilani K K Birla Goa Campus, Goa-403726, India

*Corresponding author. Tel. /fax: +91 832 2580318/25570339.

*E-mail address: naren70@yahoo.com (N. N. Ghosh)

Author's email addresses: p20180429@goa.bits-pilani.ac.in (Debika Gogoi),

priyankamakkar1991@gmail.com (Priyanka Makkar)

1. Details of Chemicals

Cobalt Nitrate $Co(NO_3)_2.6H_2O$ (Merck, India), Ferric Nitrate $Fe(NO_3)_3.9H_2O$ (Fisher Scientific), polyethylene glycol (PEG-400) (Fisher Scientific), Sodium Hydroxide (NaOH) (Fisher Scientific) were used for the synthesis of $CoFe_2O_4$ nanoparticles. Melamine (Molychem) was used for the synthesis of graphitic carbon nitride (gC_3N_4). Other chemicals used were 30% H_2O_2 (Merck, India), Methylene Blue (Fisher Scientific), Methyl Orange (Fisher Scientific), Congo Red (Loba Chemie Pvt. Ltd.), Drimaren Turquoise CL-B p (Archroma), Drimaren Yellow CL-2R p (Archroma) and Drimaren Red CL-5B p (Archroma). De-ionized water was used for all the experiments and all the chemicals were used as purchased without further purification.

2. Details of Instruments

The synthesized materials were characterized by- X-ray diffraction (XRD) by using a powder X-ray diffractometer (Mini Flex II, Rigaku, Japan) with Cu Kα (λ=0.154 nm), thermogravimetric analysis (TGA) by using a DTA-60 (Shimadzu, Japan), Field Emission Scanning Electron Microscopy (FESEM) by using Quanta 250 FEG (FEI), Energy Dispersive X-ray Spectra (EDS) by using an EDAX ELEMENT electron microscope, Fourier Transform Infrared (FT-IR) spectroscopy by using an FT-IR spectrophotometer (IR Affinity-1, Shimadzu, Japan), Raman spectroscopy by using a Horiba via Raman microscope with a 532 nm laser excitation and UV-Vis diffuse reflectance spectroscopy (DRS) by using a JASCO V-770 spectrophotometer. A 150 W Xenon lamp (400-1000 nm) was used as an irradiation source. OCT-L TOC analyser (Shimadzu, Japan) was used to determine the TOC removal ratio of dye solutions.

Table S1. Comparison of photocatalytic efficiency of 50CF-50gC_3N_4 with other gC_3N_4 based photocatalyst.

S. No.	Photocatalyst	Catalyst dose ($g\ L^{-1}$)	Dye Used	Conc. of dye solution (ppm)	Irradiation Source Xe lamp (W)	Degradation %	Time (h)	Reference
1	gC_3N_4-Bi_2WO_6	1	MO	5	300	93%	2	33
2	$BaTiO_3$@ gC_3N_4	0.5	MO	5	200	76%	6	79
3	gC_3N_4-Bi_2MoO_6	1	MO	5	300	100%	2	80
4	$MnFe_2O_4$/gC_3N_4/TiO_2	0.5	MO	10	150	99.27 %	3	71
5	$ZnAl_2O_4$/g-C_3N_4	1	MO	10	500	96%	2	81
6	gC_3N_4-$BiVO_4$	1	MO MB	5 10	300	~80% 94%	2 1.5	82
7	gC_3N_4/$ZnWO_4$	0.5	MB	3	500	94.1%	3	83
8	Graphene/ gC_3N_4	3	MB	0.2	300	77%	1.66	84
9	PANI-gC_3N_4	2	MB	10	500	92.8%	2	40
10	gC_3N_4-TiO2@PANI	0.2	CR	20	Solar light (12450-13174 Lux)	100%	3	85
11	SiO_2/gC_3N_4	2	CR	60	500	~90%	6	86
12	BN/gC_3N_4	0.5	CR	20	350	91.9%	1.5	87
13	50CF-50gC_3N_4	0.5	MB	25	150	~100%	0.75	**Our work**
14	50CF-50gC_3N_4	1	MO	10	150	~100%	1.5	**Our work**
15	50CF-50gC_3N_4	0.5	CR	25	150	~100%	1.5	**Our work**
16	50CF-50gC_3N_4	0.5	Turq CL-B	25	150	~100%	1.5	**Our work**
17	50CF-50gC_3N_4	0.5	Yell CL-2R	25	150	~100%	0.75	**Our work**
18	50CF-50gC_3N_4	0.5	Red CL-5B	25	150	~100%	1	**Our work**

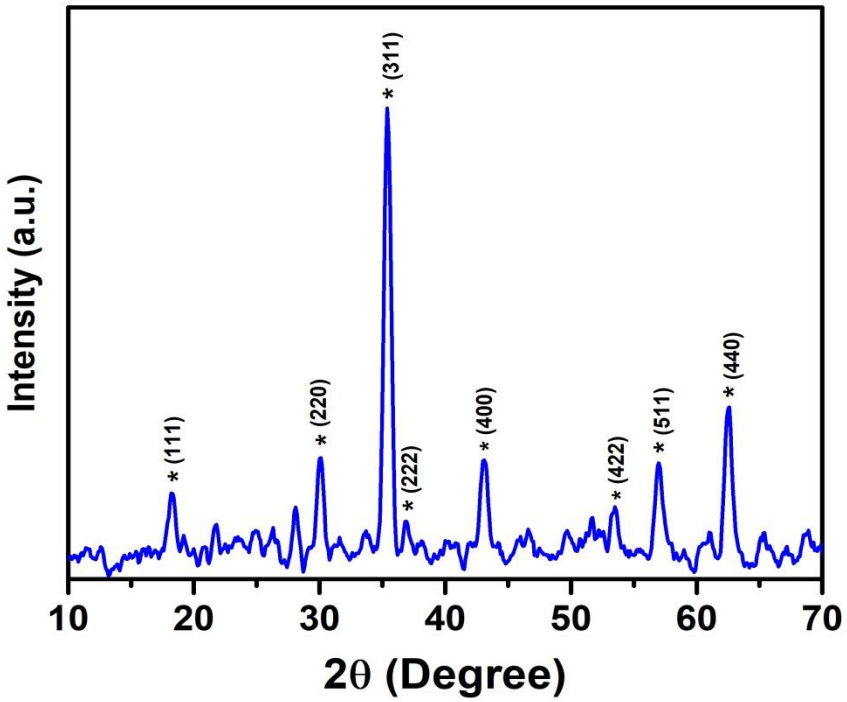

Figure S1. XRD patterns of pure $CoFe_2O_4$.

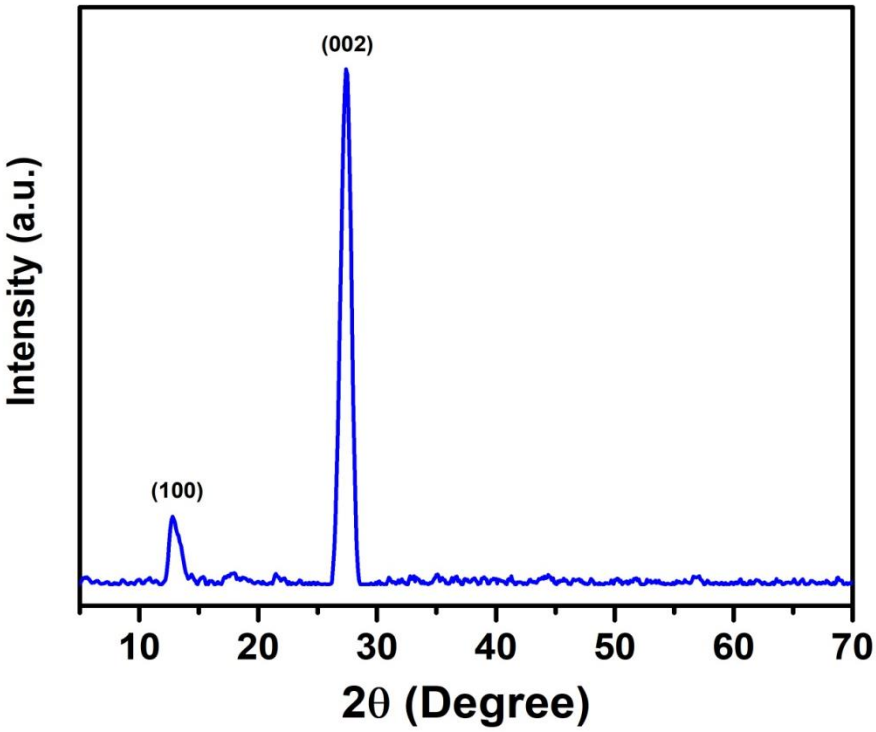

Figure S2. XRD patterns of pure gC_3N_4.

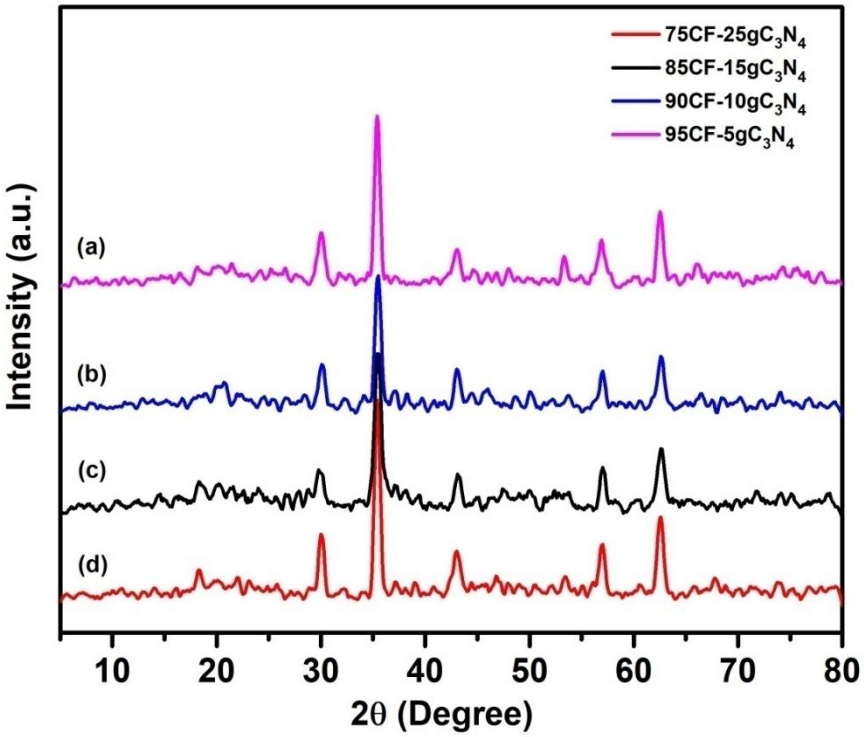

Figure S3. XRD patterns of (a) 95CF-5gC_3N_4, (b) 90CF-10gC_3N_4, (c) 85CF-15gC_3N_4 and (d) 75CF-25gC_3N_4.

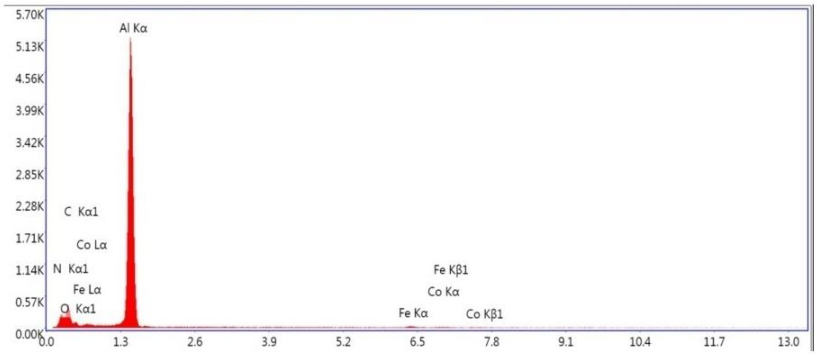

Element	Weight %	Atomic %	Net Int.	Error %	Kratio	Z	A	F
C K	19.8	28.8	22.2	12.4	0.0336	1.0808	0.1568	1.0000
N K	28.6	35.7	35.1	11.7	0.0432	1.0561	0.1428	1.0000
O K	6.2	6.7	10.3	14.9	0.0083	1.0345	0.1302	1.0000
AlK	43.9	28.4	536.2	3.2	0.3325	0.9204	0.8223	1.0006
FeK	1.0	0.3	4.0	20.9	0.0088	0.7914	1.0106	1.0948
CoK	0.4	0.1	1.5	52.5	0.0037	0.7729	1.0117	1.1142

Figure S4. EDS of 50CF-50gC_3N_4.

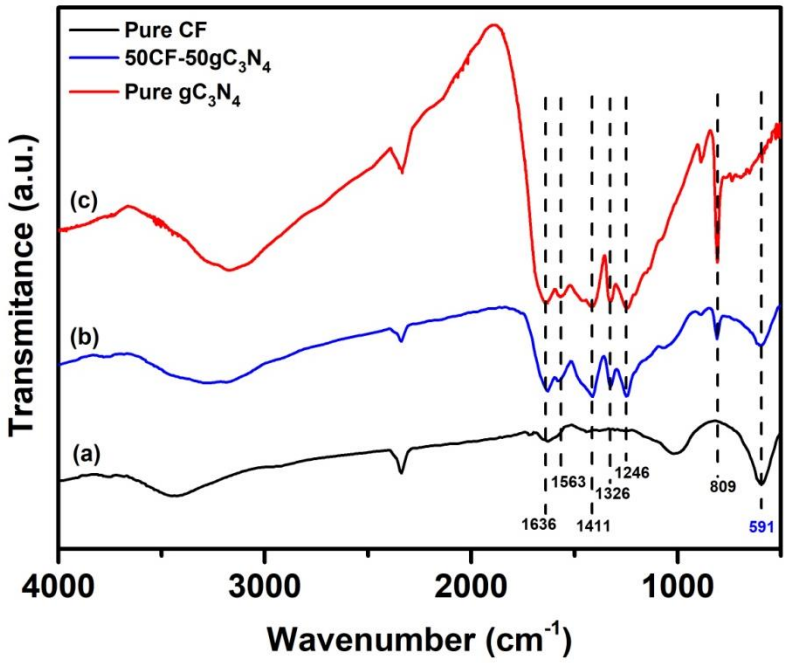

Figure S5. FT-IR spectra of (a) CF, (b) 50CF-50gC_3N_4 and (c) gC_3N_4.

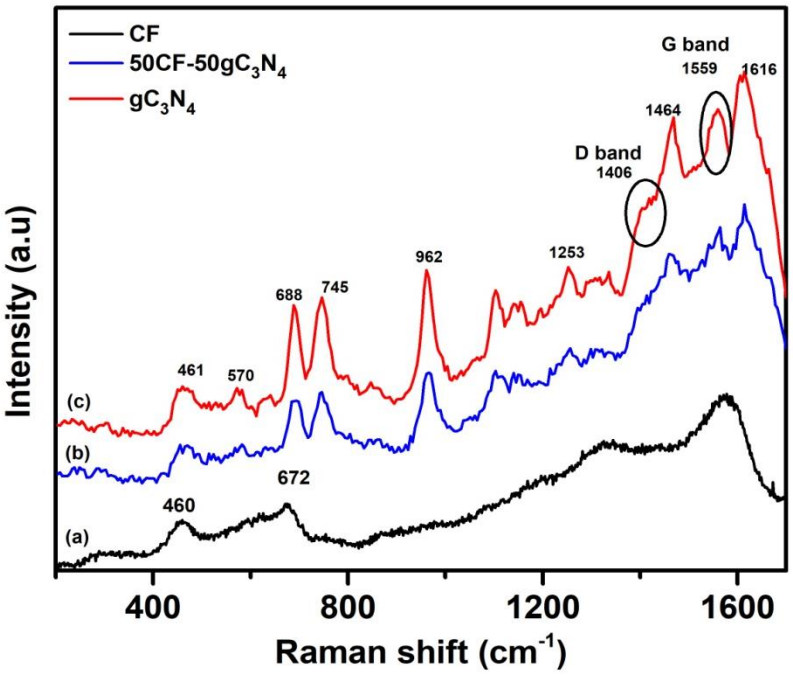

Figure S6. Raman spectra of (a) CF, (b) 50CF-50gC_3N_4 and (c) gC_3N_4.

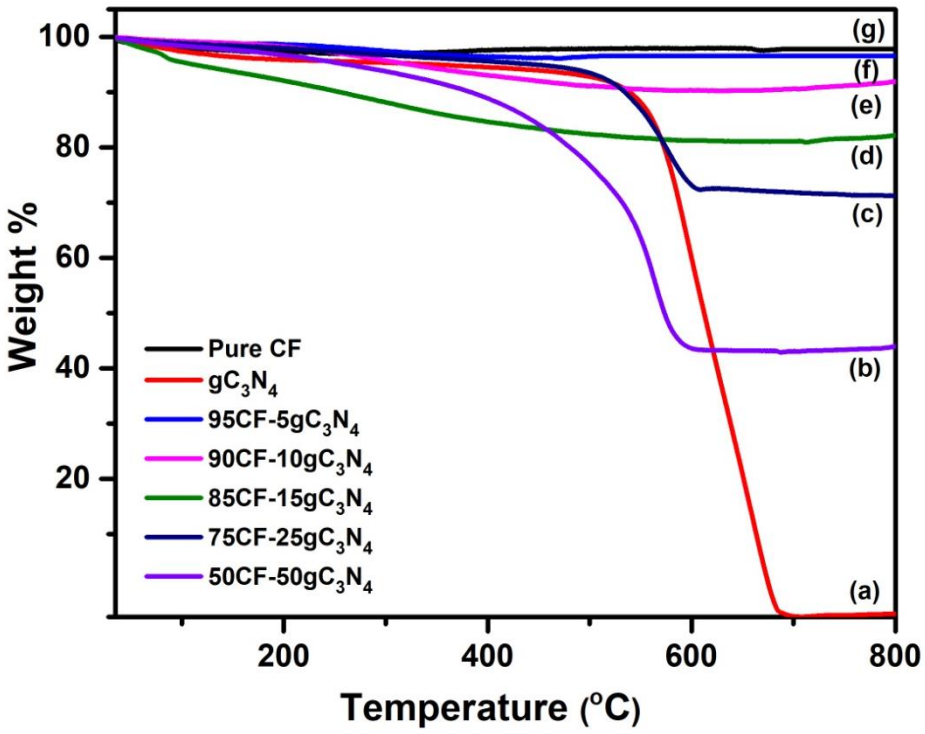

Figure S7. TGA curves of (a) Pure gC_3N_4, (b) 50CF-50gC_3N_4, (c) 75CF-25gC_3N_4, (d) 85CF-15gC_3N_4, (e) 90CF-10gC_3N_4, (f) 95CF-5gC_3N_4 and (g) Pure CF in the temperature range 35°C-800°C.

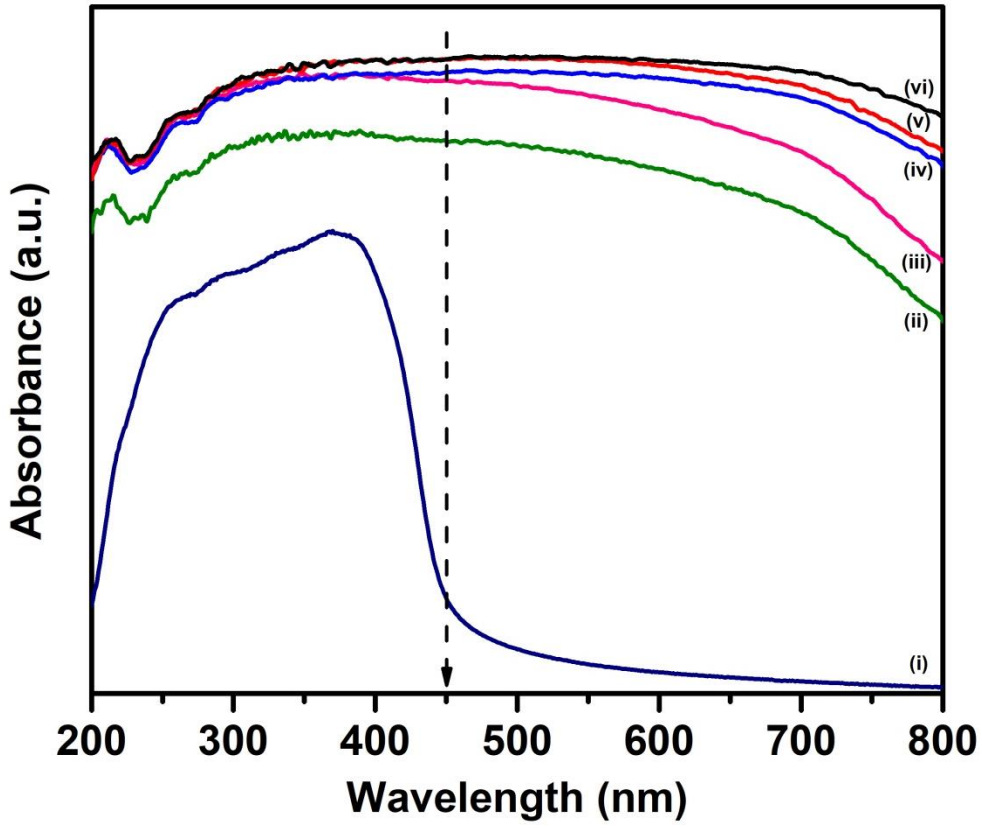

Figure S8. UV-Vis diffuse absorption spectra of (i) Pure gC_3N_4, (ii) 50CF-50gC_3N_4, (iii) 75CF-25gC_3N_4, (iv) 85CF-15gC_3N_4, (v) 90CF-10gC_3N_4, and (vi) 95CF-5gC_3N_4.

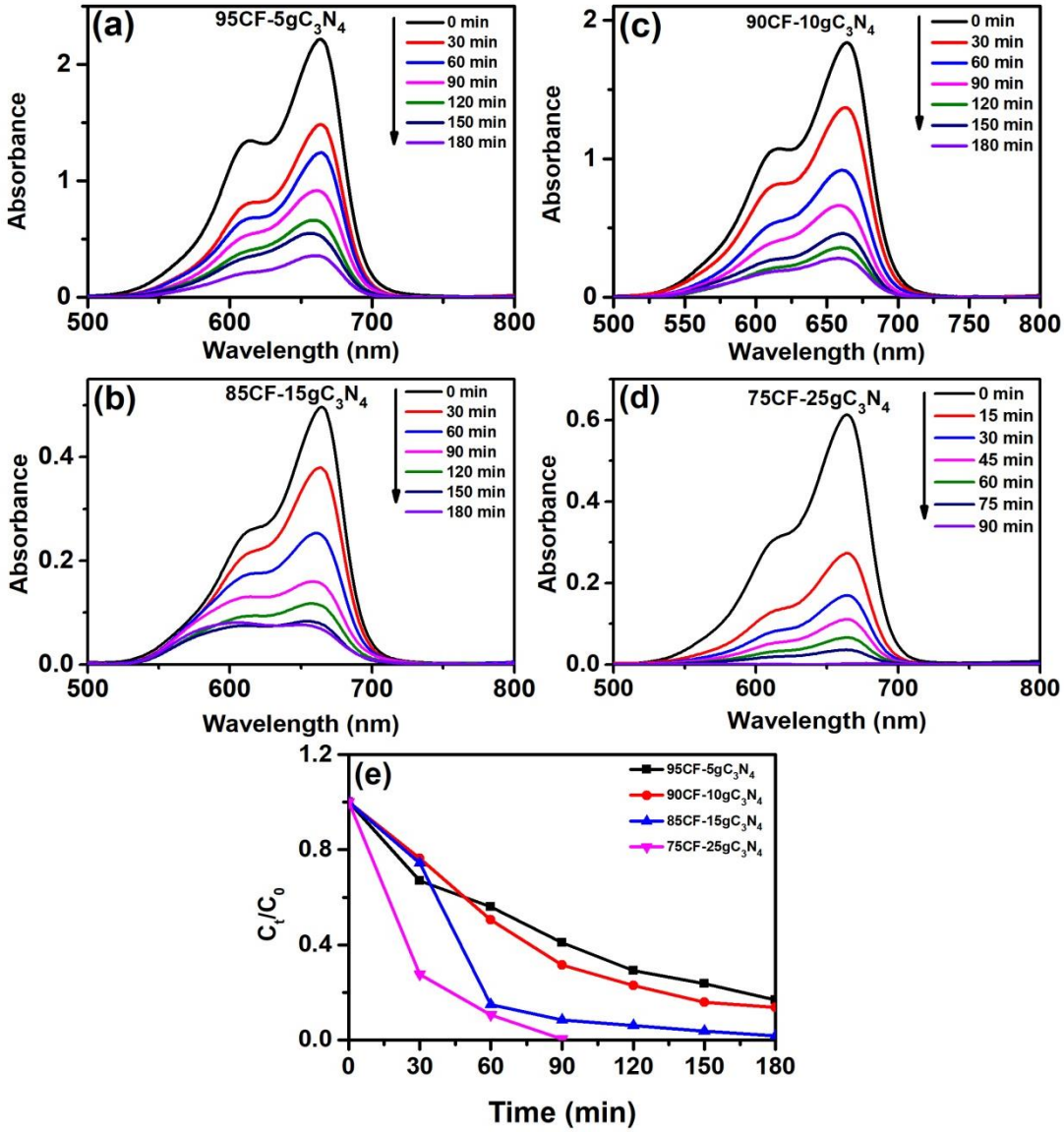

Figure S9. (a-d) Time dependent UV-Vis spectral changes of photodecomposition reaction of MB catalysed by different CF-gC_3N_4 nanocomposites (e) Photodegradation rates of the MB catalysed by different CF-gC_3N_4 nanocomposites.

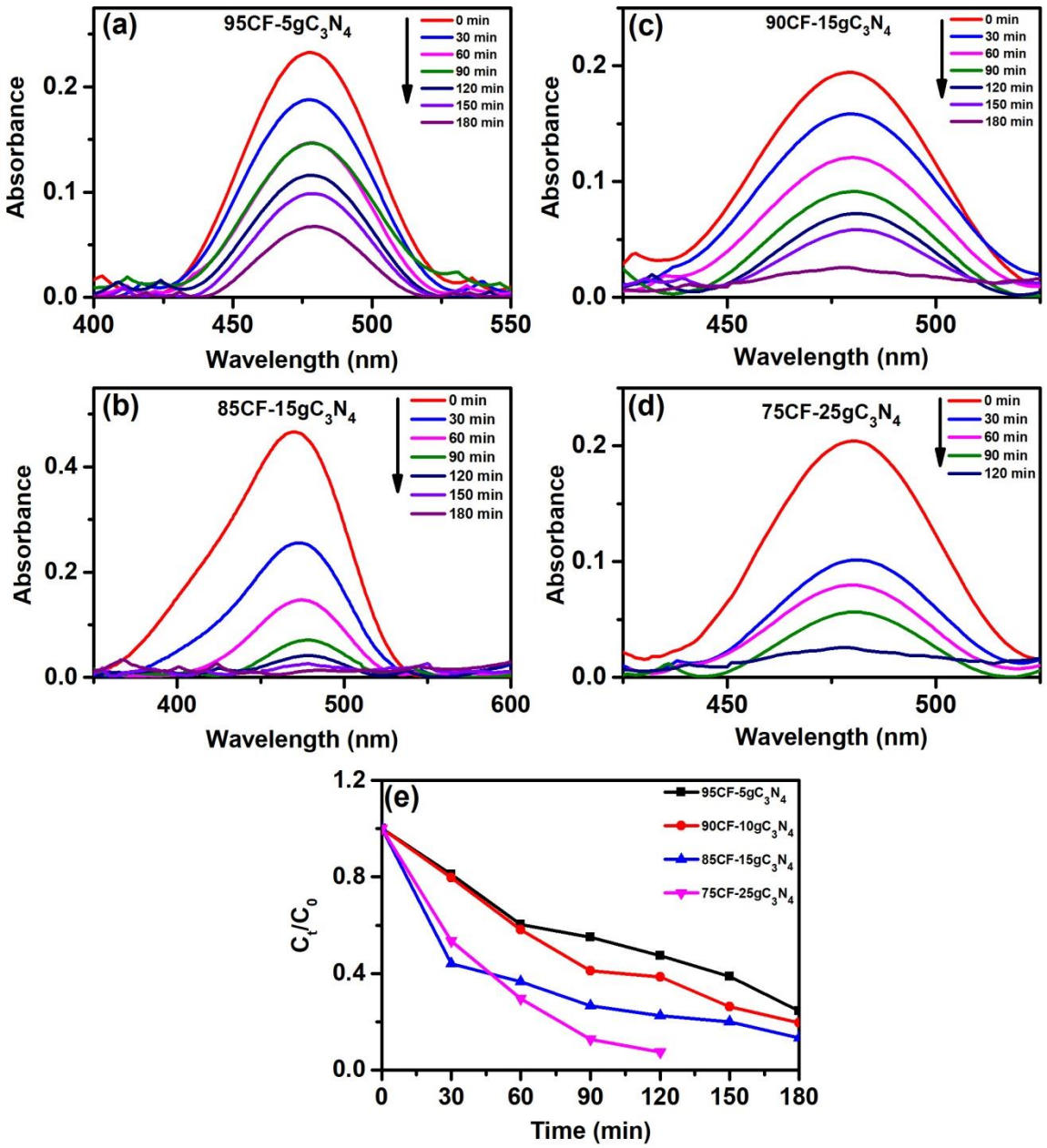

Figure S10. (a-d) Time dependent UV-Vis spectral changes of photodecomposition reaction of MO catalysed by different CF-gC_3N_4 nanocomposites (e) Photodegradation rates of the MO catalysed by different CF-gC_3N_4 nanocomposites.

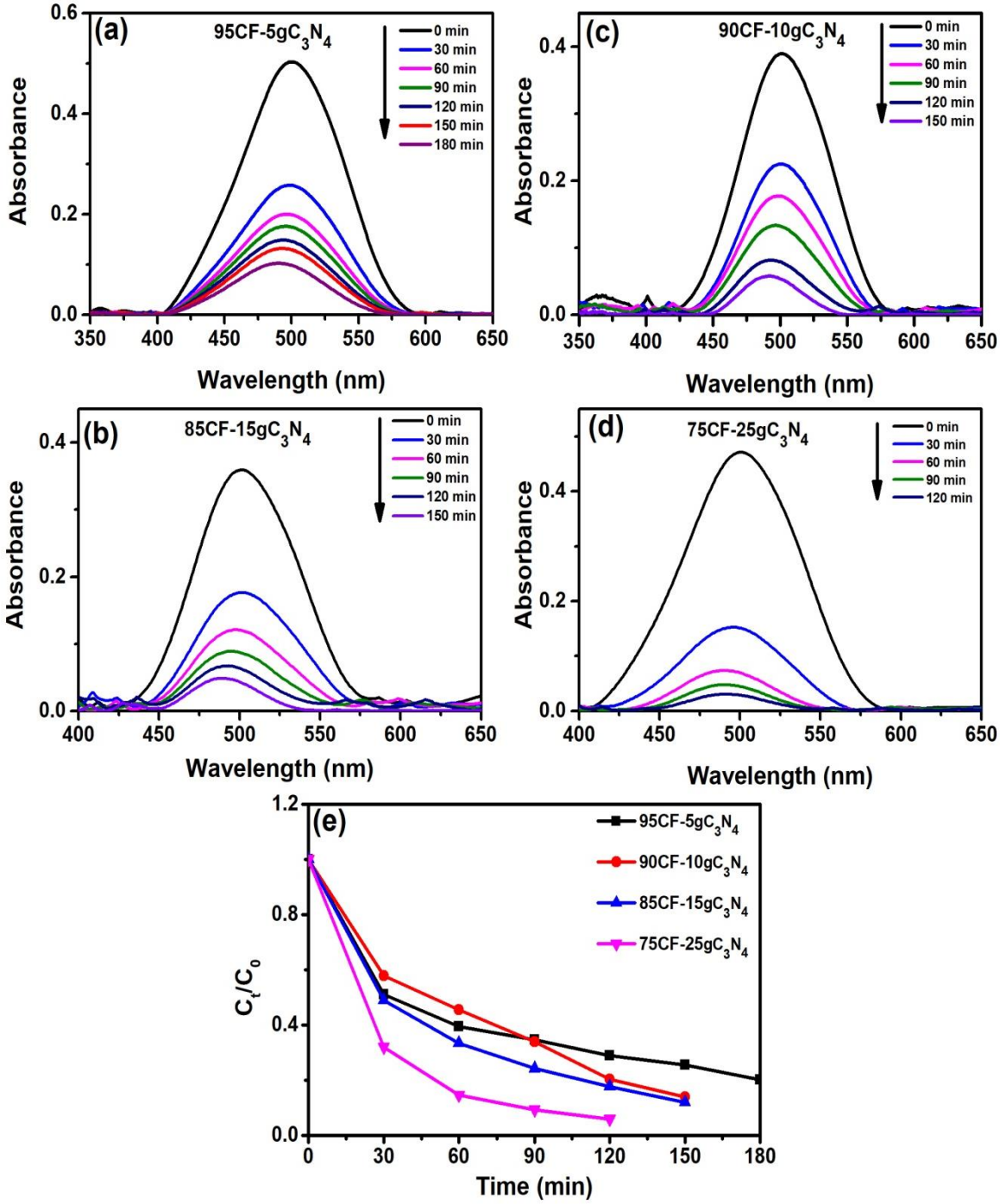

Figure S11. (a-d) Time dependent UV-Vis spectral changes of photodecomposition reaction of CR catalysed by different CF-gC_3N_4 nanocomposites (e) Photodegradation rates of the CR catalysed by different CF-gC_3N_4 nanocomposites.

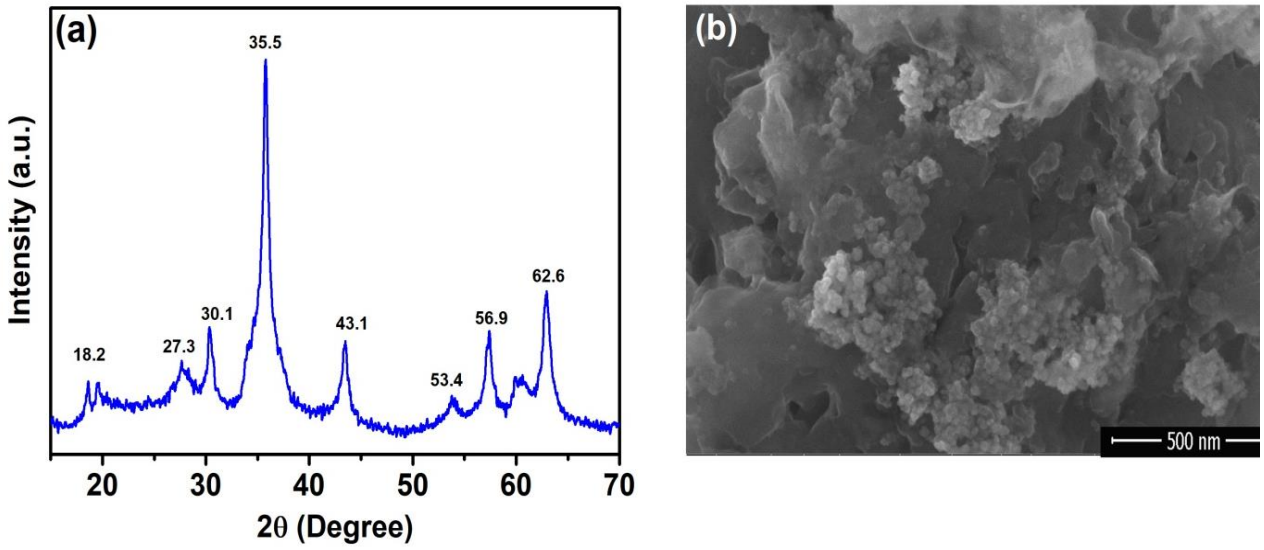

Figure S12. (a) XRD plot, (b) FESEM image of the used 50CF-50gC_3N_4 catalyst.